HHS Public Access

Author manuscript

Free Radic Biol Med. Author manuscript; available in PMC 2018 November 01.

Published in final edited form as:

Free Radic Biol Med. 2017 November ; 112: 131–140. doi:10.1016/j.freeradbiomed.2017.07.015.

Enzymatic and Free Radical Formation of *Cis*- and *Trans*-Epoxyeicosatrienoic Acids *In Vitro* and *In Vivo*

Theresa Aliwarga[a], **Brianne S. Raccor**[b], **Rozenn N. Lemaitre**[c], **Nona Sotoodehnia**[c,d], **Sina A. Gharib**[e], **Libin Xu**[a], and **Rheem A. Totah**[a,*]

[a]Department of Medicinal Chemistry, University of Washington, Box 357610, Seattle, WA 98195, USA

[b]Department of Pharmaceutical Sciences, Campbell University, PO Box 1090, Buies Creek, NC 27506, USA

[c]Cardiovascular Health Research Unit, Department of Medicine, University of Washington, 1730 Minor Ave, Suite 1360, Seattle, WA 98101, USA

[d]Division of Cardiology, University of Washington, Box 356422, Seattle, WA 98195, USA

[e]Computational Medicinal Core, Center for Lung Biology, Division of Pulmonary & Critical Care Medicine, Department of Medicine, University of Washington, S376- 815 Mercer, Box 385052, Seattle, WA 98109, USA

Abstract

Epoxyeicosatrienoic acids (EETs) are metabolites of arachidonic acid (AA) oxidation that have important cardioprotective and signaling -6 polyunsaturated fatty acid (PUFA) that is prone to autoxidation. Although hydroperoxides and isoprostanes are major autoxidation products of AA, EETs are also formed from the largely overlooked peroxyl radical addition mechanism. While autoxidation yields both cis- and trans-EETs, cytochrome P450 (CYP) epoxygenases have been shown to exclusively catalyze the formation of all regioisomer cis-EETs, on each of the double bonds. In plasma and red blood cell (RBC) membranes, cis- and trans-EETs have been observed, and both have multiple physiological functions. We developed a sensitive ultra-performance liquid chromatography tandem mass spectrometry (UPLC-MS/MS) assay that separates cis- and trans-isomers of EETs and applied it to determine the relative distribution of cis- vs. trans-EETs in reaction mixtures of AA subjected to free radical oxidation in benzene and liposomes in vitro. We also determined the in vivo distribution of EETs in several tissues, including human and mouse heart, and RBC membranes. We then measured EET levels in heart and RBC of young mice

*Corresponding Author: Rheem A. Totah, 206-543-9481 (Telephone), 206-685-3252 (Fax), rtotah@uw.edu.

Author contributions: T.A. and B.S.R designed and performed experiments, analyzed and interpreted data, wrote and edited manuscript. R.N.L, N.S, and S.A.G provided samples, designed experiments and edited manuscript. L.X. and R.A.T provided materials, designed experiment, interpreted data, wrote and edited manuscript.

Competing interests: The authors declare that there is no conflict of interest.

Data and materials availability: Data are available upon request to the corresponding author.

compared to old. Formation of EETs in free radical reactions of AA in benzene and in liposomes exhibited time- and AA concentration-dependent increase and trans-EET levels were higher than cis-EETs under both conditions. In contrast, cis-EET levels were overall higher in biological samples. In general, trans-EETs increased with mouse age more than cis-EETs. We propose a mechanism for the non-enzymatic formation of cis- and trans-EETs involving addition of the peroxyl radical to one of AA's double bonds followed by bond rotation and intramolecular homolytic substitution (SHi). Enzymatic formation of cis-EETs by cytochrome P450 most likely occurs via a one-step concerted mechanism that does not allow bond rotation. The ability to accurately measure circulating EETs resulting from autoxidation or enzymatic reactions in plasma and RBC membranes will allow for future studies investigating how these important signaling lipids correlate with heart disease outcomes.

Graphical abstract

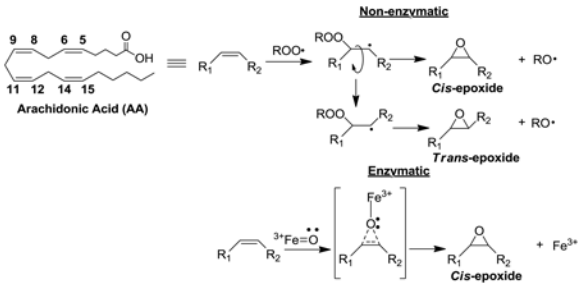

Keywords

cis-EETs; trans-EETs; free radical oxidation; arachidonic acid; RBC; heart; CYP2J2; lipid peroxidation; oxidative stress; epoxygenase

Introduction

Poly unsaturated fatty acids (PUFAs) are highly susceptible to free radical oxidation commonly known as lipid peroxidation. A comprehensive discussion of reactions involved in lipid peroxidation has been reviewed by Yin et al. [1]. Oxidative stress, associated with various disease states, perturbs the balance of reactive oxygen species (ROS), which in turn leads to increased lipid peroxidation. Briefly, the process originates in the formation of lipid radical followed by generation of lipid peroxyl radical with molecular oxygen addition. The peroxyl radical can propagate the chain reactions by either abstracting a hydrogen atom from another lipid molecule or adding to a double bond of another (Fig. 1). The radical formed after the addition tends to undergo intramolecular homolytic substitution (S_Hi) to give an epoxide and an alkoxyl radical that continues the chain reaction. Detailed mechanism of peroxyl radical addition reactions has been discussed by Xu et al. [2]. Lipid peroxidation *in vivo* has been linked to the underlying pathophysiology of various disease states, including atherosclerosis, myocardial ischemia-reperfusion injury, diabetes, cancer, and neurodegenerative injury [3-7].

Arachidonic acid (AA) is an essential ω-6 PUFA found mainly esterified at the *sn2*-position of phospholipids. Like other PUFAs, AA is highly susceptible to lipid peroxidation leading to several compounds including hydroperoxides and isoprostanes [1]. Almost all products of AA autoxidation reported previously were derived from the hydrogen atom-transfer peroxidation mechanism due to the high reactivity of AA as a hydrogen atom donor at the *bis*-allylic position. In constrast, limited information is available on the peroxyl radical addition pathway during AA autoxidation, which is the focus of this report.

Release of AA from membranes is tightly regulated *in vivo* and is calcium-dependent. Upon activation of phospholipase A_2, AA is hydrolyzed from phospholipids and subject to oxidation through various pathways, including the CYP pathway (Fig. 2). It is well established that AA can be metabolized by various CYP isoforms to all regioisomers of physiologically active *cis*- EETs among other hydroxyl metabolites [8, 9]. EETs play several crucial roles especially in the cardiovascular system, including modulating vascular tone by activating calcium-sensitive potassium channels which in turn promotes hyperpolarization and relaxation of smooth muscle cells, attenuating inflammatory process by inhibiting pro-inflammatory transcription factor, nuclear factor-κB (NF-κB), and improving post-ischemic-reperfusion injury by enhancing ventricular repolarization recovery [10, 11].

Both *cis*- and *trans*-EETs detected in RBC membranes and plasma are mostly esterified in phospholipid membranes [12-14]. In fact, RBC membranes have been proposed as a reservoir of *cis*- and *trans*-EETs that can be formed through CYP oxidation, by hemoglobin, or by free radical oxidation [13, 15, 16]. Like *cis*-EETs, *trans*-EETs are biologically active and have been shown to relax preconstricted rat arcuate arteries [14]. They are also hydrolyzed to dihydroxy metabolites at a higher rate than *cis*-EETs by soluble epoxide hydrolase [13]. To date, the relative importance of *cis*- vs. *trans*-EETs in cardioprotection and their relative distribution in different biological samples from diseased patients have not been reported.

Here we developed an UPLC-MS/MS method capable of separating *cis*- and *trans-geometric* isomers of all EET regioisomers and determined the product distribution of EETs formed through free radical oxidation in benzene and in liposomes *in vitro.* We also measured the *cis*- and *trans*-EETs distribution in several tissues *in vivo,* including mouse heart tissue and RBC of young and old mice, as well as human heart tissue and RBC. We further propose a mechanism for non-enzymatic formation of *cis*- and *trans*-EETs. Finally, *in vitro* CYP incubation conditions with AA were optimized using CYP2J2 as a model isozyme. ROS scavengers were varied to inhibit autoxidation of AA and more accurately determine CYP metabolite profile and product distribution.

Materials and Methods

Reagents

Stocks of AA, *cis*-EETs (14,15-, 11,12-, 8,9-, and 5,6-EETs), deuterated internal standards (14,15-EET-d_{11}, 8,9-EET-d_{11}, 5,6-EET-d_{11}, and 14,15-DHET-d_{11}) and 4-[[*trans*-4-[[(tricyclo[3.3.1.$1^{3,7}$]dec-1-ylamino)carbonyl]amino]cyclohexyl]oxy]-benzoic acid (*t*-AUCB) were purchased from Cayman Chemical (Ann Arbor, MI). 2,2′-azobis(4-

methoxy-2,4-dimethylvaleronitrile) (MeOAMVN) and 2,2′-azobis(2-(2-imidazolin-2-yl) propane) dihydrochloride (AIPH) were obtained from Wako Chemicals USA, Inc (Richmond, VA). Pure AA stocks were purchased from Nu-Chek-Prep, Inc (Elysian, MN). Dulbecco's phosphate buffered saline (PBS), ACS-grade ethyl acetate, chloroform, Optima-grade acetonitrile, water, and methanol were purchased from Fisher Scientific (Hampton, NH). Benzene, triphenylphosphine (TPP), butylated hydroxytoluene (BHT), phospholipase A_2 from *Naja mossambica mossambica,* pyruvic acid, and diethylenetriaminepentaacetic acid (DETAPAC) were obtained from Sigma-Aldrich (St. Louis, MO). 1,2-dilauryl-*sn*-glycero-3-phosphocholine (DLPC) and 1,2-dioleoyl-*sn*-glycero-3-phosphocholine (DOPC) were purchased from Avanti Polar Lipids, Inc (Alabaster, AL).

Free radical oxidation of AA in benzene

The total reaction volume was 200 μL. Pure AA was reconstituted in benzene that was filtered through neutral alumina. The stock solution of AA (164.2 mM) was diluted in benzene to obtain 1, 10, 25, and 50 mM solutions. The reaction was then initiated with addition of MeOAMVN (10 μL, 0.03 M) and incubated at 37°C in a sand bath for 1, 2, or 3 h. At the end of each time point, the reaction was terminated by adding BHT (50 μL, 0.2 M) and TPP (50 μL, 0.2 M) in benzene at room temperature. For the zero-time point, the reaction was immediately terminated after addition of AA. Samples were cooled to room temperature and a 10 μL aliquot was mixed with 10 μL of internal standard solution (a mixture of d_{11}- 14,15-, 8,9-, 5,6-EETs and d_{11}-14,15-DHET in benzene, 3 μg/mL each). Samples were dried under nitrogen at 25°C followed by reconstitution in 1 mL of 50% of water and 50% of 80:20 acetonitrile:methanol. Samples were then analyzed on the same day by LC-MS as described below.

Free radical oxidation of AA in liposomes

Free radical oxidation of AA in liposomes was achieved following a procedure by Xu et. al. [17]. Briefly, chloroform solutions of DLPC (20 μL, 250 mM), of DOPC (n_{OA} 0 to 0.76), and of AA (n_{AA} 0 to 0.76) were mixed together so that the concentration of total fatty acyl chains remain constant. The mixtures were dried under nitrogen at 25°C and kept under vacuum for 10 min. The dried samples were reconstituted in PBS and sonicated for 20 sec. The suspension was incubated at 37°C for 10 min followed by another cycle of 20 second sonication. The free radical oxidation was initiated by addition of AIPH (10 μL, 20 mM). Addition of BHT (50 μL, 0.2 M) and TPP (50 μL, 0.2 M) terminated the reaction at room temperature. After 30 min, internal standards (10 μL, a mixture of d11- 14,15-, 8,9-, 5,6-EETs and d11-14,15-DHET in 1× PBS, 3 μg/mL each) were added. The EETs were then extracted twice using nitrogen-purged ethyl acetate containing 0.1 mM TPP. The ethyl acetate extracts were combined and dried under nitrogen at 25°C. The dried residue was reconstituted using 1 mL of a solution containing 50% of water and 50% of 80:20 acetonitrile:methanol. The samples were then analyzed on the same day by LC-MS.

Mouse erythrocyte membranes and heart tissue

C57BL/6 mice (N=14, 10 females and 4 male) were purchased from Charles River Laboratories. These mice were separated into two groups based on their age. Mice that were approximately 5 month old or younger were categorized into the young group, while mice

that were between 18.3 to 22.5 months of age were categorized into the old group. Whole blood from mice was collected through cardiac puncture following CO_2 treatment. The collected blood was washed three-times with cold 1 × PBS and stored at -80°C until processed further. After removal of heart tissue from the chest cavity of the mouse, the tissue was immediately washed with cold 1 × PBS and flash frozen in liquid nitrogen. All animal experiments were performed in compliance with approved protocols by Institutional Animal Care and Use Committee of the University of Washington.

Human erythrocyte membranes and heart tissue

Human erythrocyte membrane samples were population-based control samples from a repository of sudden cardiac arrest cases and controls. In this study, we used a random sample of 28 controls that had been collected between October 1988 and September 2005 as part of a case-control study of erythrocyte fatty acids and incident sudden cardiac arrest [18]. The University of Washington Human Subject Review Committee approved the study protocol. Discarded nonischemic and ischemic human heart residual tissues were obtained from University of Washington Medical Center as surgical waste during cardiac transplants and other procedures. Ventricular tissues were immediately flash-frozen in liquid nitrogen and stored at -80°C until further processing.

Extraction of EETs from erythrocyte membranes

Methods to extract RBC and cardiac tissue EETs were modified from published protocols [12, 19]. Each tissue was extracted in duplicates. Briefly, for erythrocyte membranes, 498 μL of deionized water and 2 μL of internal standard (a mixture of d_{11}- 14,15-, 8,9-, 5,6-EETs and d_{11}-14,15-DHET, 3 μg/mL each) were added to 0.5 mL of RBC membranes containing 50 mg/mL total protein for human and 30 mg/mL total protein for mouse. The samples were centrifuged at 3,500 rpm for 5 min at 4°C. The RBC samples were extracted using 4 mL of 2:1 chloroform:methanol containing 0.1 mM TPP, followed by rotary mixing for one hour at 4°C. The mixture was then centrifuged at 3,500 rpm for 15 minutes at 4°C to remove cellular debris. The chloroform layer was dried under nitrogen at 25°C, followed by addition of 50 mM Tris-HCl, 100 mM NaCl, 1 mM $CaCl_2$ buffer, pH 9.2 containing 10 units of phospholipase A_2 from *Naja Mossambica Mossambica* (1 mL). The samples were incubated for 30 minutes at 37°C to hydrolyze EETs from the membrane. The EETs were extracted twice with nitrogen-purged ethyl acetate containing 0.1 mM TPP (2 × 2mL), and the ethyl acetate fractions were pooled and evaporated to dryness under nitrogen at 25oC. The lipid residue was reconstituted in 10 μL of DMSO to ensure complete dissolution of EETs and 40 μL of a solution containing 50% of water and 50% of 80:20 acetonitrile:methanol, respectively. The samples were then analyzed directly by LC-MS.

Extraction of EETs from cardiac tissue

EET extraction from cardiac tissue was initiated by homogenizing the cardiac tissue in 490 μL of cold 1× PBS in the presence of 12.1 μM *t*-AUCB, a soluble epoxide hydrolase inhibitor, and six ceramic beads using Precellys24 (Bertin Instruments, Rockville, MD) at 6800 rpm for 6 × 30 seconds with 60 seconds delay between cycles. Prior to dividing the homogenized tissue into duplicate aliquots of 100 μL, 10 μL of internal standards (a mixture of 14,15-EET-d_{11}, 8,9-EET- d_{11}, 5,6-EET-d_{11}, and 14,15-DHET-d_{11}, 3 μg/mL each) were

added to each sample of the homogenized tissue. The rest of the EET extraction protocol from the cardiac tissue followed similar procedure for EET extraction from RBC above. All extractions were performed in duplicates.

In vitro incubation using reconstituted CYP enzyme system

In vitro experiments were performed using recombinantly expressed and purified CYP2J2 [20]. Reconstituted enzyme system consisted of purified CYP2J2 (25 pmol), cytochrome P450 reductase, and cytochrome b5 in a ratio of 1:2:1, respectively in 50 μg/mL of extruded DLPC (500 μL total incubation volume). The buffer was 100 mM potassium phosphate buffer, pH 7.4 containing 0.1 mM DETAPAC. Following addition of NADPH (1.0 mM), the samples were pre-equilibrated at 37°C for 3 min after which the reaction was initiated with 50 μM AA containing 1 mM pyruvate. After 30 minutes, reactions were terminated with 2 mL of nitrogen-purged ethyl acetate containing 0.01% BHT to minimize non-enzymatic AA oxidation and a mixture of internal standards (1 μg/mL of 14,15-EET-d_{11}, 8,9-EET-d_{11}, and 5,6-EET-d_{11}, 3 μg/mL each) was added. The quenched reactions were vortexed rigorously for 10 minutes followed by centrifugation at 3500 rpm at 4°C for 5 min. The ethyl acetate extraction was performed twice, the organic layers were combined and evaporated to dryness under a gentle stream of nitrogen at room temperature. The residue was reconstituted with 10 μL of DMSO and 40 μL of a solution containing 50% of water and 50% of 80:20 acetonitrile:methanol, respectively. Samples were analyzed using LC-MS-MS on the same day.

Liquid chromatograph and mass spectrometric assay to quantify EETs

Quantification of *cis*- and *trans*-EETs was performed on a Waters Xevo TQ-S triple quadrupole mass spectrometer operated in negative ion mode electrospray coupled to a Waters UPLC. The EETs were separated on a Waters Acquity UPLC® BEH Shield RP C18 1.7 μm, 100 × 2.1 mm column. Several columns with various stationary and bonded phase using UPLC system were compared. The Agilent Zorbax SB-C18, Rapid resolution HT, 2.1×50 mm with 1.8 μicron particle size was used. This column had no end-capping with 10% carbon load, 80 Å pore size and 180 m^2/g surface area. The chromatographic resolution of individual EET was not satisfactory because there were not enough theoretical plates on this column. We switched to the current Waters Acquity UPLC® BEH Shield RP18, 2.1×100 mm with 1.7 μm particle size. The length of the column and a slight increase in the particle size of the column's stationary phase provided improved chromatographic resolution. The end-capping appeared to improve the chromatography.

The mobile phase water containing 0.05% acetic acid (solvent A) and 80:20 acetonitrile: methanol containing 0.05% acetic acid (solvent B). The various isomers of EETs were separated using the following gradient: solvent B was held at 62% from 0 to 5.5 min, then held at 55% from 5.5 to 6 min, followed by an increase to 58% from 6 to 18 min, and finally increased to 100% from 18.1 to 19.1 min. Solvent B was then held at 62% from 20 to 23 min to re-equilibrate the column. Flow rate was constant at 0.3 mL/min throughout the run. For the first 2 min of runtime, 100% of the flow was diverted into waste. The MS conditions were the following: capillary voltage 2 kV, cone voltage 20 V, source temperature 150°C, desolvation temperature 450°C. The mass transitions that were monitored are 319.1 >219.1

(14,15-EET), 319.1>208 (11,12-EET), 319.1>166.7 (11,12-EET), 319.1>155.1 (8,9-EET), 319.1>191.2 (5,6-EET) and compared to their corresponding deuterated standards. For 11,12-EET, 14,15-EET-d_{11} was used as the internal standard.

In the absence of authentic standards, *trans*-EETs were identified based on retention time, fragmentation pattern and comparison to methods previously published [15]. To further confirm the presence and identity of *trans*-EETs, a free radical oxidation sample that contained 50 mM AA and oxidized for 3 hours in liposomes was analyzed using High Resolution/High Mass Accuracy Thermo LTQ-OrbiTrap, which confirmed the identity of the peaks presumed as *trans*-EETs came from the same parent ions and had the same fragmentation patterns as their corresponding *cis*-EET (Fig. S1).

Data analysis

Mass spectrometry data were analyzed using MassLynx 4.1. Data analysis was performed using Prism 5.04 (GraphPad, La Jolla, CA). In the free radical oxidation study, experiments were performed in triplicates and reported as the mean ± S.D. Mass transition 319.1>208 was used to obtained peak area ratio for 11,12-EET. Experiments measuring EETs from biological samples were reported as means ± standard deviations.

Integrated peak area of each analyte was normalized to the corresponding peak area of internal standard. In addition to analyte normalization to its internal standard, the normalized peak areas of each analyte at the zero time-point were subtracted from the corresponding peak areas of each sample.

In optimization of *in vitro* incubation using reconstituted CYP enzyme system, experiments were performed in duplicates. In this subset of data, analyte peak height, instead of peak area, was used and further normalized to its internal standard. As mentioned above, two mass transitions were monitored for 11,12-EET; 319.1>166.7 and 319.1>208. The peak intensity of 11,12-EET at 319.1>166.7 was higher than 319.1>208 even though chromatographic separation between 11,12-EET and 8,9-EET at mass transition 319.1>166.7 was not at baseline level. Peak height was used to quantitatively measure 11,12-EET for another set of experiment. The percentage of non-NADPH-dependent EETs was obtained by taking ratio of the normalized peak height of no-NADPH control and the normalized peak height of corresponding sample that contained NADPH.

Results

Free radical oxidation of AA in benzene or liposomes leads to formation of both *cis*- and *trans*-EETs

Free radical oxidation of AA at various concentrations (ranging from 1 to 50 mM) was initiated by MeOAMVN at 37 °C and the formation of *cis*- and *trans*- EETs was monitored at different time points using UPLC-MS/MS. In addition to the major hydroxyl metabolites, both *cis*- and *trans*-EETs were formed in this reaction (Fig. S2). Formation of c*is*- and *trans*-EETs was linear with respect to time- and AA concentration for all regioisomers in benzene with Fig. 3A-D demonstrating this relationship for 14,15-EET and Fig. S3-S4 showing all other regioisomers. Furthermore, for all conditions, *trans*-EETs formation was favored over

cis-EETs formation by approximately 1.5 to 6.2 fold (Fig. 3E, Fig. 4A, and Fig S5). The percentage of each isomer of EET (regio- or stereo- isomer) to total EETs formed remained relatively constant at different AA concentrations and various time points as summarized in Table 1.

To study radical formation of EETs in a more physiologically relevant system, oxidation of AA was performed in liposomes. The reaction contained a constant mole fraction of DLPC while varying mole fractions of oxidizable phospholipid, DOPC, and AA, so that the total moles of fatty acyl chain remains constant in the incubation. Free radical oxidation was initiated with water-soluble radical initiator, AIPH, at 37°C. Similar to radical reactions in benzene, *cis*- and *trans*-EETs formation was linear with time- and mole fraction of AA in liposomes for all regioisomers. The linear formation of 14,15-EET is shown as an example in Fig. 5A-D with other regioisomers shown in Fig. S6 and Fig. S7. The ratio of each regioisomer of EET relative to total EETs remained unchanged for both *cis*- and *trans*-EETs at various concentrations of AA and at various time points (Fig. 5E and Fig S8). The formation of *trans*-EETs was also favored in liposomes by approximately 2.5 and 10.5 over *cis*-EETs formation (Fig. 5E, Fig. 4B, and Fig. S8). Compared to free radical oxidation in solution (i.e. benzene), more variability was observed in reactions in liposomes. At 1 mM of AA (n_{AA} of 0.015), the levels of both *cis*- and *trans*-EETs were similar to those observed in benzene. However, the formation of EETs in the presence of liposomes at higher concentration of AA was more efficient than in benzene as seen in Fig. 5A-B and Fig. S6-S7. Regardless of the difference in product distribution between benzene and liposome oxidations, the percentages of each regioisomer of EETs relative to total EETs was also relatively unaltered across all conditions (concentration and time) in liposome as seen in Table 1 (Bottom half).

Product distribution of cis- and *trans*- EETs in biological samples

Extraction of EETs from erythrocyte membranes of C57BL/6 mice and humans revealed the presence of both geometric isomers of all EET regioisomers (Fig. 6). In contrast to the free radical oxidation reactions, *cis*-EETs are higher than *trans*-EETs in RBC membranes as evidenced by the larger normalized peak-height ratios in Table 2 and 3. The ratios of *cis*-/*trans*-EETs for each regioisomer ranged from 0.9 to 2.2 for old mouse RBC membranes (N=7), 1.3 to 4.0 for young mouse RBC membranes (N=7), and 1.0 to 3.1 for human RBC membranes (N=28). The ratios of *trans*-/*cis*-total EETs in old mouse RBCs are significantly higher than those in young mouse RBCs, suggesting increased contribution of the free radical mechanism to *trans*-EETs with aging (Fig. 7). In general, for each EET pair, the *cis*-/*trans*- ratios in RBC membranes of both old mouse and human are similar. However, the *cis*-/*trans*- ratios of 8,9- and 5,6-EETs in young mouse RBC membranes are significantly larger than those in old mouse and human RBC membranes.

The ratios of *cis*-/*trans*-EETs for each regioisomer from mouse heart tissues ranged from 0.38 to 1.3 (N=7), while the ratios from human heart tissues ranged from 0.80 to 2.8 (N=12). In mouse heart tissues, the levels of *cis*-14,15- and *cis*-5,6-EETs were similar to their *trans*-EETs while the levels of *cis*-11,12- and *cis*-8,9-EETs were significantly lower than their

trans-counterparts (Table 2). In diseased human heart tissues, the levels of all four *cis*-EETs were higher than their corresponding *trans*-EETs (Table 3).

In vitro enzymatic and non-enzymatic formation of *cis*- and *trans*- EETs

CYP2J2 was chosen as a model CYP epoxygenase since it is capable of generating all four regioisomers of *cis*-EETs and at approximately similar amounts [21]. In a CYP2J2 reconstituted system including Cytochrome P450 oxidoreductase and cytochrome b5, both *cis*-and *trans*- regioisomers of EETs were observed in the presence and absence of NADPH (Fig.8), suggesting contribution from both enzymatic and autoxidation processes. We sought to establish conditions that would diminish, if not eliminate, the non-NADPH dependent formation of EETs during CYP incubations to facilitate accurate metabolite identification and kinetic studies of various fatty acids. Thus, we investigated the effect of an iron-chelating agent, DETAPAC, and hydrogen peroxide scavenger, pyruvate, at various concentrations. Table 4 shows percentage of remaining EETs that were formed in non-NADPH-dependent manner in the presence of each protective reagent. Spectrometric binding studies were conducted and confirmed that neither pyruvate or DETAPAC bind to the CYP2J2 active site and had no effect on the iron spin state (data not shown).

Discussion

EETs have been implicated in many biological processes and play an important role in cardioprotection. We sought to determine the contribution of autoxidation to the formation of *cis*- and *trans*-EETs both in benzene and in liposomes, a more physiologically relevant system. The key finding of this study is that EETs are readily formed from AA under free radical oxidation conditions. All regio- and geometric isomers were formed. The percentage of each *cis*- or *trans*-EET to total EETs did not change with increasing concentration of AA or with time whether reactions were carried out in benzene or liposomes. However, the percentages of both *cis*- and *trans*-14,15- and 5,6-EETs were significantly different between solution and liposome reactions. Formation of 14,15-EET appeared to be less favored in liposomes than in solution while the formation of 5,6-EET seemed to be more favored in liposomes. It is possible that the heterogeneous environment of liposomes contributes to 5,6-EET formation. The double bond at the C5 position is much closer to the carboxylic acid group than the double bond at the C14 position. In the presence of liposomes, AA would be more likely to bury its hydrophobic tail; therefore, access to the double bond at the C14 position would be slightly restricted by lipid peroxyl radicals and oxidation will be more favorable at the 5,6-position. Similar regio-distribution of oxidation products of linoleic acid in liposomes has been reported previously, where formation of C9-isomers are preferred over C13-isomers [17].

The ratios of *cis*- to *trans*-EETs from free radical oxidation are in general higher in benzene than in liposomes as shown in Figures 3E and 5E. Irrespective of the reaction medium, formation of *trans*-EETs was favored over *cis*-EETs. In contrast, levels of *cis*-EETs were, in general, either more favored or similar to *trans*-EETs depending on the specific regioisomer pairs in biological samples, such as human and mouse RBC membranes or human and mouse heart tissues. Of note, a considerably higher ratio of *cis*-/*trans*-8,9-EETs was

observed in human heart tissues compared to both young and old mouse heart tissues (Tables 2 and 3). This may be due to the diseased nature of the human heart tissue available to us, compared to the mouse tissue. However, further studies using healthy human heart tissue will be necessary to confirm this observation.

In mouse RBC, both total *cis*- and *trans*-EETs increased in RBC of old mice as seen in Fig. 7, but *trans*-EETs increased to a much larger extent. Aging is associated with progressive endothelial dysfunction [27,28], defective vascular repair [28], arterial thickening and stiffness [29], angiogenesis impairment [30], an increased risk of developing atherosclerosis [31], and an accumulation of senescent endothelial cells [32]. Yang et. al. showed that the endothelial function was gradually reduced in 6-week, 20-week, and 80-week Sprague-Dawley rats and addition of exogenous *cis*-14,15-EET improved endothelial function in aging mice as well as endothelial senescence in rat mesenteric arterial endothelial cells from 20-week-old rat through mTORC2/Akt signaling pathway [33]. 11,12-EET also attenuated inflammation by reducing phenylephrine-induced constriction and increasing endothelial-dependent dilation of aortic rings from 22-month-ovariectomized Norway rats and decreasing cytokine-stimulated upregulation of adhesion molecules on human aortic endothelial cells [34]. However, in 6-week 129 SvJ mouse model, 8,9- and 5,6-EETs had been shown to promote angiogenesis and *de novo* vascularization while 14,15- and 11,12-EETs did not exhibit the same mitogenic properties [35]. All aforementioned studies demonstrated that all EETs had protective properties, however, each regioisomer of EET required different biological pathways to be activated to promote cell proliferation. In pulmonary murine microvascular endothelial cells, 8,9- or 11,12-EETs had been shown to be involved in activation of p38 MAPK, whereas mitogenic activity of 5,6- or 14,15-EETs had been reported to be mediated by PI3-kinase/Akt signaling [35]. Because aging is progressively complicated processes, any negative effect of aging could compromise various downstream signaling pathways involved in cell proliferation. These compromised pathways could alter the level of EETs, especially *trans*-EETs were primarily formed via free radical oxidation process and warrant measurement of both the *cis*- and *trans*-isomers.

Presence of all four *cis*- regioisomer of EETs in human RBC membranes was shown by Nakamura et al., but the authors did not report the presence of both *cis* and *trans* isomers [15]. In the analytical method developed in this study, both the *cis*- and *trans-EETs* present in RBC membranes were easily resolved (Fig. 6), which enabled their detection for the first time. While we clearly demonstrated that both geometric isomers of EETs are observed in the RBC membranes of mouse and human, their origin is less certain. EETs, both *cis*- and *trans-,* could potentially result from various sources, including enzymatic CYP or hemoglobin oxidation of hydrolyzed AA, or free radical oxidation of either free AA or AA esterified to phospholipids in the membrane.

CYP epoxygenases are known to only form *cis*-EETs (Fig. 8K-T) while autoxidation of AA leads to formation of both *cis*- and *trans-EETs* with preference to *trans*-regioisomers (Fig. 8A-E) [8,9]. The most likely mechanism of *trans-EETs* formation is through a peroxyl radical addition mechanism [1,2]. Peroxyl radical addition to any of the double bonds of AA leads to the formation of a carbon radical, which could directly undergo S_Hi reaction to give

the *cis*-EETs, or undergo S_Hi after rotation of the σ bond to give the *trans*-EETs as proposed in Fig. 9.

Another potential mechanism is the *cis-trans* isomerization of AA prior to free radical oxidation or enzyme catalysis. Roy et al. reported that certain *trans* double bonds of AA lead to formation of *trans-EETs* in CYP-catalyzed reactions [22]. The process of *cis*- to *trans*-AA isomerization can be mediated by nitrogen dioxide, a free radical byproduct of nitric oxide and nitrite oxidation or thiyl radicals [23,24]. However, these mechanisms are unlikely to occur under *in vitro* reaction conditions. On the other hand, in CYP-mediated reactions, the iron-oxo species (or potentially the hydroperoxy species) catalyzes the epoxide formation in a one-step concerted mechanism that does not allow for bond rotation and formation of *trans*-EETs [25].

Owing to the fact that EETs are formed from autoxidation of AA, it is important to optimize *in vitro* CYP incubation conditions to minimize the contribution from autoxidation. This will ensure that formation of *cis*-EETs observed in the presence of NADPH are mediated exclusively by CYP catalysis. Thus, we tested several approaches to minimize autoxidation without affecting enzymatic activity. In *in vitro* systems, non-NADPH-dependent EETs are potentially generated from Fenton chemistry. Therefore, addition of iron-chelating agents, EDTA or DETAPAC, markedly inhibited the formation of EETs from autoxidation. Another major uncoupling product of CYP catalysis is hydrogen peroxide, which can initiate the P450 cycle and also lead to EETs formation. To circumvent this reaction, pyruvate was also added to scavenge hydrogen peroxide [26]. Combination of both, iron-chelating agent and pyruvate efficiently inhibited the majority of EET formation from autoxidation as shown in Table 4. In addition, all incubations were performed in the dark to avoid photooxidation and all analyses by UPLC-MS/MS were performed immediately following quenching of reactions to minimize oxidation and degradation of metabolites.

Conclusion

Lipid peroxidation is involved in the pathophysiology of various human disorders including cardiovascular disease. Oxidative stress during these disease states leads to the increase of reactive oxygen species, which increases lipid peroxidation due to the susceptibility of unsaturated lipids to oxidation. Autoxidation of AA has been previously reported to form hydroperoxides, isoprostanes, and monohydroxylated metabolites. In this study, we report EETs as another important class of products readily formed from AA autoxidation. Non-enzymatic *trans*-EETs are formed more favorably via free radical oxidation mechanisms, while CYP epoxygenases contribute to the formation of *cis*-EETs. A number of studies have measured EETs in plasma of cardiovascular disease patients compared to healthy volunteers, however, future efforts should focus on determining if one (or more) geometic isomer is more likely to vary during cardiovascular disease. In this manner, the contribution of both free radical and enzymatic oxidation to the total circulating EET pool can be assessed leading to a better understanding of the protective roles played by each regioisomer, and establishing whether certain regio- or geometric- isomers can serve as potential biomarkers for specific cardiovascular conditions.

Supplementary Material

Refer to Web version on PubMed Central for supplementary material.

Acknowledgments

The authors thank Dr. Nahush A. Mokadam from the Division of Cardiothoracic surgery at University of Washington and Dr. Jean C. Dinh from Children's Mercy Hospital for establishing our human heart bank, Dale Whittington and J. Scott Edgar for their expertise and assistance in mass spectrometric analysis.

Funding: This work was supported in part by National Institute of Health Grants R01HL130880, R01HL088456 and R01HL096706.

References

1. Ying H, Xu L, Porter NA. Free radical lipid peroxidation: mechanisms and analysis. Chem Rev. 2011; 111(10):5944–72. https://doi.org/10.1021/cr200084z. [PubMed: 21861450]
2. Xu L, Porter NA. Free radical oxidation of cholesterol and its precursors: Implications in cholesterol biosynthesis disorders. Free Radic Res. 2015; 49(7):835–849. https://doi.org/10.3109/10715762.2014.985219. [PubMed: 25381800]
3. Shao B, Heinecke JW. HDL, lipid peroxidation, and atherosclerosis. J Lipid Res. 2009; 50(4):599–601. https://doi.org/10.1194/jlr.E900001-JLR200. [PubMed: 19141435]
4. Lucas DT, Szweda LI. Cardiac reperfusion injury: aging, lipid peroxidation, and mitochondrial dysfunction. Proc Natl Acad Sci USA. 1998; 95(2):510–514. [PubMed: 9435222]
5. Davi G, Falco A, Patrono C. Lipid peroxidation in diabetes mellitus. Antioxid Redox Signal. 2005; 7(1-2):256–268. https://doi.org/10.1089/ars.2005.7.256. [PubMed: 15650413]
6. Barrera G. Oxidative stress and lipid peroxidation products in cancer progression and therapy. ISRN Oncol. 2012; 2012:137289. https://doi.org/10.5402/2012/137289. [PubMed: 23119185]
7. Abeti R, Parkinson MH, Hargreaves IP, Angelova PR, Sandi C, Pook MA, Giunti P, Abramov AY. Mitochondrial energy imbalance and lipid peroxidation cause cell death in Friedreich's ataxia. Cell Death Dis. 2016; 7:e2237. https://doi.org/10.1038/cddis.2016.111. [PubMed: 27228352]
8. Oliw EH, Guengerich FP, Oates JA. Oxygenation of arachidonic acid by hepatic monooxygenases. Isolation and metabolism of four epoxide intermediates. J Biol Chem. 1982; 257(7):3771–3781. [PubMed: 6801052]
9. Oliw EH. Oxygenation of polyunsaturated fatty acids by cytochrome P450 monooxygenases. Prog Lipid Res. 1994; 33(3):329–354. [PubMed: 8022846]
10. Yang L, Maki-Petaja K, Cheriyan J, McEniery C, Wilkinson LB. The role of epoxyeicosatrienoic acids in the cardiovascular system. Br J Clin Pharmacol. 2015; 80(1):28–44. https://doi.org/10.1111/bcp.12603. [PubMed: 25655310]
11. Batchu SN, Law E, Brocks DR, Falck JR, Seubert JM. Epoxyeicosatrienoic acid prevents postischemic electrocardiogram abnormalities in an isolated heart model. J Mol Cell Cardiol. 2009; 46(1):67–74. https://doi.org/10.1016/j.yjmcc.2008.09.711. [PubMed: 18973759]
12. Jiang H, McGiff JC, Quilley J, Sacerdoti D, Reddy LM, Falck JR, Zhang F, Lerea KM, Wong PY. Identification of 5,6-trans-epoxyeicosatrienoic acid in the phospholipids of red blood cells. J Biol Chem. 2004; 279(35):36412–36418. https://doi.org/10.1074/jbc.M403962200. [PubMed: 15213230]
13. Jiang H, Zhu AG, Mamczur M, Morisseau C, Hammock BD, Falck JR, McGiff JC. Hydrolysis of cis- and trans- epoxyeicosatrienoic acids by rat red blood cells. J Pharmacol Exp Ther. 2008; 326(1):330–337. https://doi.org/10.1124/jpet.107.134858. [PubMed: 18445784]
14. Jiang H, Quilley J, Doumad AB, Zhu AG, Falck JR, Hammock BD, Stier CT Jr, Carroll MA. Increases in plasma trans-EETs and blood pressure reduction in spontaneously hypertensive rats. Am J Physiol Heart Circ Physiol. 2011; 300(6):H1990–H1996. https://doi.org/10.1152/ajpheart.01267.2010. [PubMed: 21398593]

15. Nakamura T, Bratton DL, Murphy RC. Analysis of epoxyeicosatrienoic and monohydroxyeicosatetraenoic acids esterified to phospholipids in human red blood cells by electrospray tandem mass spectrometry. J Mass Spectrom. 1997; 32(8):888–896. https://doi.org/10.1002/(SICI)1096-9888(199708)32:8<888::AID-JMS548>3.0.CO;2-W. [PubMed: 9269087]
16. Jiang H, Anderson GD, McGiff JC. Red blood cells (RBCs), epoxyeicosatrienoic acids (EETs) and adenosine triphosphate (ATP). Pharmacol Rep. 2010; 62(3):468–474. [PubMed: 20631410]
17. Xu L, Davis TA, Porter NA. Rate constants for peroxidation of polyunsaturated fatty acids and sterols in solution and in liposomes. J Am Chem Soc. 2009; 131(36):13037–13044. https://doi.org/10.1021/ja9029076. [PubMed: 19705847]
18. Siscovick DS, Raghunathan TE, King I, Weinmann S, Wicklund KG, Albright J, Bovbjerg V, Arbogast P, Smith H, Kushi LH, Cobb LA, Copass MK, Psaty BM, Lemaitre R, Retzlaff B, Childs M, Knopp RH. Dietary intake and cell membrane levels of long-chain n-3 polyunsaturated fatty acids and the risk of primary cardiac arrest. JAMA. 1995; 274(17):1363–1367. [PubMed: 7563561]
19. Goulitquer S, Dreano Y, Berthou F, Corcos L, Lucas D. Determination of epoxyeicosatrienoic acids in human red blood cells and plasma by GC/MS in the NICI mode. 2008; 876(1):83–88. https://doi.org/10.1016/j.jchromb.2008.10.035.
20. Evangelista EA, Kaspera R, Mokadam NA, Jones JP 3rd, Totah RA. Activity, inhibition, and induction of cytochrome P450 2J2 in adult human primary cardiomyocytes. Drug Metab Dispos. 2013; 41(12):2087–2094. https://doi.org/10.1124/dmd.113.053389. [PubMed: 24021950]
21. Kaspera R, Totah RA. Epoxyeicosatrienoic acids: formation, metabolism and potential role in tissue physiology and pathophysiology. Expert Opin Drug Metab Toxicol. 2009; 5(7):757–771. https://doi.org/10.1517/17425250902932923. [PubMed: 19505190]
22. Roy U, Loreau O, Balazy M. Cytochrome P450/NADPH-dependent formation of trans epoxides from trans-arachidonic acids. Bioorg Med Chem Lett. 2004; 14(4):1019–1022. https://doi.org/10.1016/j.bmcl.2003.11.054. [PubMed: 15013014]
23. Jiang H, Kruger N, Lahiri DR, Wang D, Vatele JM, Balazy M. Nitrogen dioxide induces cis-trans-isomerization of arachidonic acid within cellular phospholipids. Detection of trans-arachidonic acids in vivo. J Biol Chem. 1999; 274(23):16235–16241. [PubMed: 10347179]
24. Ferreri C, Samadi A, Sassatelli F, Landi L, Chatgilialoglu C. Regioselective cis-trans isomerization of arachidonic double bonds by thiyl radicals: the influence of phospholipid supramolecular organization. J Am Chem Soc. 2004; 126(4):1063–1072. https://doi.org/10.1021/ja038072o. [PubMed: 14746474]
25. Vaz ADN, McGinnity DF, Coon MJ. Epoxidation of olefins by cytochrome P450: evidence from site-specific mutagenesis for hydroperoxo-iron as an electrophilic oxidant. Proc Natl Acad Sci USA. 1998; 95(7):3555–3560. [PubMed: 9520404]
26. Long LH, Halliwell B. Artefacts in cell culture: pyruvate as a scavenger of hydrogen peroxide generated by ascorbate or epigallocatechin gallate in cell culture media. Biochem Biophys Res Commun. 2009; 388(4):700–704. https://doi.org/10.1016/j.bbrc.2009.08.069. [PubMed: 19695227]
27. Celermajer DS, Sorensen KE, Spiegelhalter DJ, Georgakopoulos D, Robinson J, Deanfield JE. Aging is associated with endothelial dysfunction in healthy men years before age-related decline in women. J Am Coll Cardiol. 1994; 24(2):471–476. [PubMed: 8034885]
28. Weinsaft JW, Edelberg JM. Aging-associated changes in vascular activity: a potential link to geriatric cardiovascular disease. Am J Geriatr Cardiol. 2001; 10(6):348–354. [PubMed: 11684920]
29. Lakatta EG, Levy D. Arterial and cardiac aging: major shareholders in cardiovascular disease enterprises: Part 1: aging arteries: a “set up” for vascular disease. Circulation. 2003; 107(1):139–146. [PubMed: 12515756]
30. Rivard A, Fabre JE, Silver M, Chen D, Murohara T, Kearney M, Magner M, Asahara T, Isner JM. Age-dependent impairment of angiogenesis. Circulation. 1999; 99(1):111–120. [PubMed: 9884387]
31. Weingand KW, Clarkson TB, Adams MR, Bostrom AD. Effects of age and/or puberty on coronary artery atherosclerosis in cynomolgus monkeys. Atherosclerosis. 1986; 62(2):137–144. [PubMed: 3801081]

32. Erusalimsky JD, Kurz DJ. Cellular senescence in vivo: its relevance in ageing and cardiovascular disease. Exp Gerontol. 2005; 40(8-9):634–642. https://doi.org/10.1016/j.exger.2005.04.010. [PubMed: 15970413]

33. Yang C, Pan S, Yan S, Li Z, Yang J, Wang Y, Xiong Y. Inhibitory effect of 14,15-EET on endothelial senescence through activation of mTOR complex2/Akt signaling pathways. Int J Biochem Cell Biol. 2014; 50:93–100. https://doi.org/10.1016/j.biocel.2014.02.020. [PubMed: 24607498]

34. Sun C, Simon SI, Foster GA, Radecke CE, Hwang HV, Zhang X, Hammock BD, Chiamvimonvat N, Knowlton AA. 11,12-Epoxyeicosatrienoic acids mitigate endothelial dysfunction associated with estrogen loss and aging: role of membrane depolarization. J Mol Cell Cardiol. 2016; 94:180–188. https://doi.org/10.1016/j.yjmcc.2016.03.019. [PubMed: 27079253]

35. Pozzi A, Marcias-Perez I, Abair T, Wi S, Su Y, Zent R, Falck JR, Capdevila JH. Characterization of 5,6- and 8,9- epoxyeicosatrienoic acids (5,6- and 8,9-EET) as potent in vivo angiogenic lipids. J Biol Chem. 2005; 280(29):27138–27146. https://doi.org/10.1074/jbc.M501730200. [PubMed: 15917237]

Abbreviations

EET	epoxyeicosatrienoic acid
AA	Arachidonic acid
PUFA	polyunsaturated fatty acid
UPLC-MS/MS	ultra-performance liquid chromatography tandem mass spectrometry
ROS	reactive oxygen species
NF-κB	nuclear factor -κB
RBC	red blood cell
***t*-AUCB**	4-[[*trans*-4-[[(tricyclo[3.3.1.1^{3,7}]dec-1-ylamino)carbonyl]amino]cyclohexyl]oxy]-benzoic acid (*t*-AUCB)
MeOAMVN	2,2′-azobis(4-methoxy-2,4-dimethylvaleronitrile)
AIPH	2,2′-azobis(2-(2-imidazolin-2-yl) propane) dihydrochloride
PBS	Dulbecco's phosphate buffered saline
TPP	triphenylphosphine
BHT	butylated hydroxytoluene (BHT)
DETAPAC	diethylenetriaminepentaacetic acid
DLPC	1,2-dilauryl-*sn*-glycero-3-phosphocholine
DOPC	1,2-dioleoyl-*sn*-glycero-3-phosphocholine
n_{AA}	mole fraction of AA

n_{OA}	mole fraction of oleic acid
KPi	potassium phosphate
HETE	hydroxyeicosatetraenoic acid

Highlights

- Both *cis*- and *trans*-EETs were readily formed in free radical oxidation.
- Formation of *trans*-EETs is more favored in free radical oxidation.
- CYP2J2 forms only *cis*-EETs.
- Levels of *cis*-EETs are generally higher in biological samples.
- In general, *trans*-EETs increased to a much higher extend than *cis*-EETs in RBC of older mice compared to younger mice.

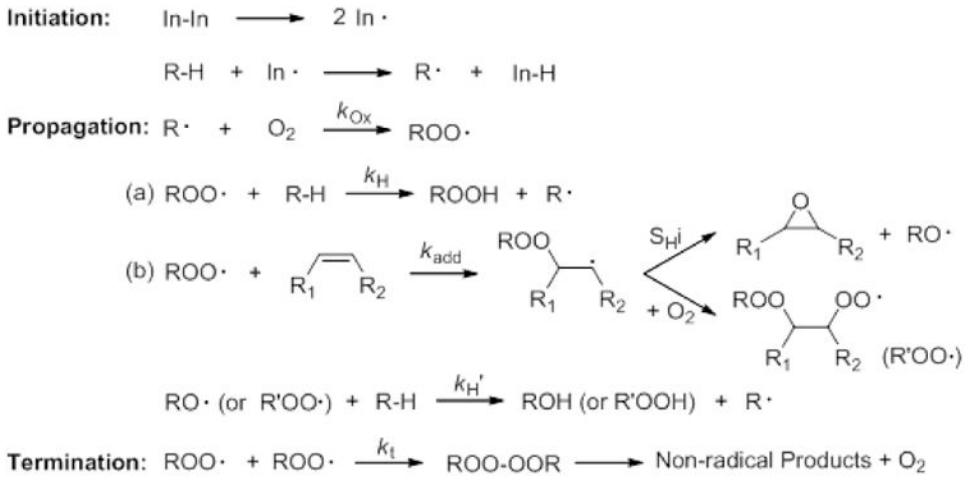

Fig 1.

Free radical chain oxidation reaction and generation of epoxides by peroxyl radical addition.

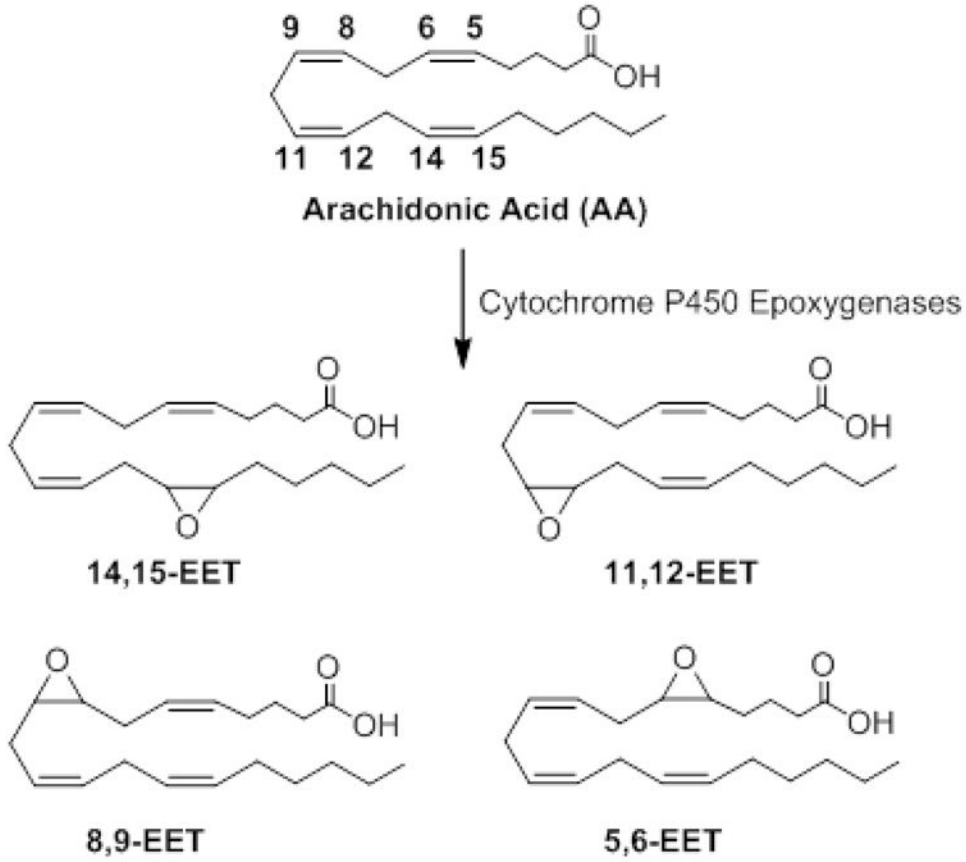

Fig. 2.

AA metabolic pathway mediated by CYP epoxygenases to form all regioisomers of *cis*-EETs

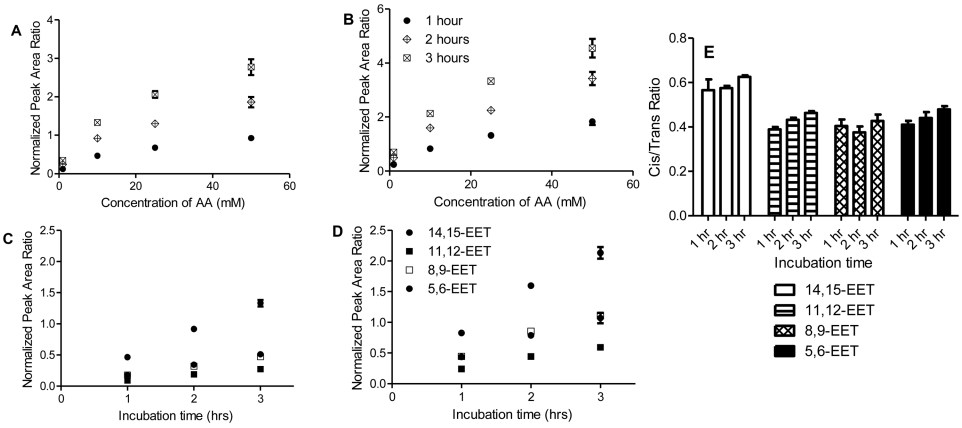

Fig. 3.

Concentration- and time-dependent formation of non-enzymatic EETs and ratio of *cis/trans*-EETs from AA in benzene. Concentration-dependent formation of non-enzymatic (A) *cis*-14,15-EET, (B) *trans*-14,15-EET. Time-dependent formation of non-enzymatic (C) *cis*-EETs, (D) *trans*-EETs at 10 mM AA. (E) Ratios of *cis*- to *trans*-EETs in benzene in the presence of 10 mM AA at various incubation time points remain unaltered. For this subset of experiments, each time point reaction was performed in triplicates and normalized to its zero-time point. Each data point shows mean ± S.D.

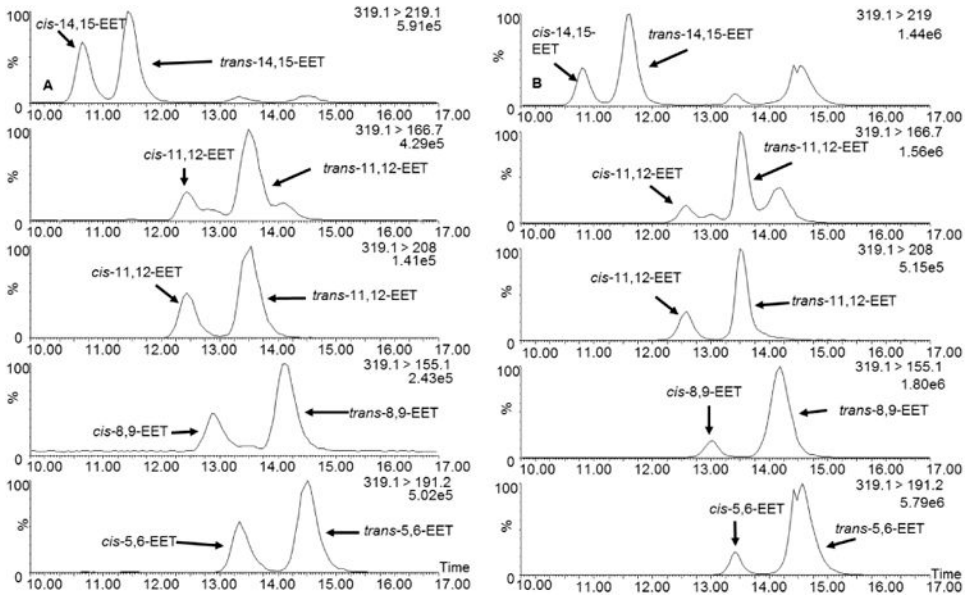

Fig. 4.

Extracted ion chromatograms of EETs formed during free radical oxidation in benzene (A) and liposomes (B). The chromatograms demonstrate separation of *cis*- and *trans*-EETs.

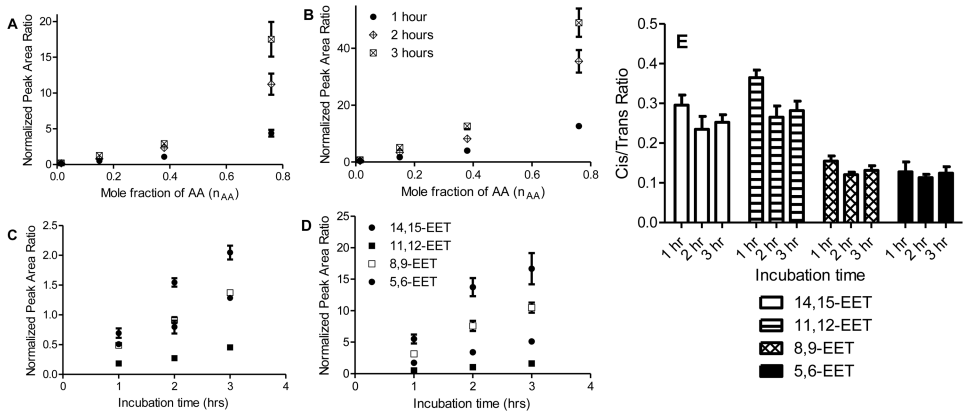

Fig. 5.

Mole fraction- and time-dependent formation of non-enzymatic EETs and ratio of *cis/trans*-EETs from AA in liposomes. Mole fraction-dependent formation of non-enzymatic (A) *cis*-14,15-EET, (B) *trans*-14,15-EET. Time-dependent formation of non-enzymatic (C) *cis*-EETs, (D) *trans*-EETs at n_{AA} of 0.15. (E) Ratios of *cis*- to *trans*-EETs in liposomes at various incubation time points and at n_{AA} of 0.15 did not change significantly. For this subset of experiment, each time point reaction was performed in triplicates and normalized to its zero time point. Each data point shows mean ± S.D.

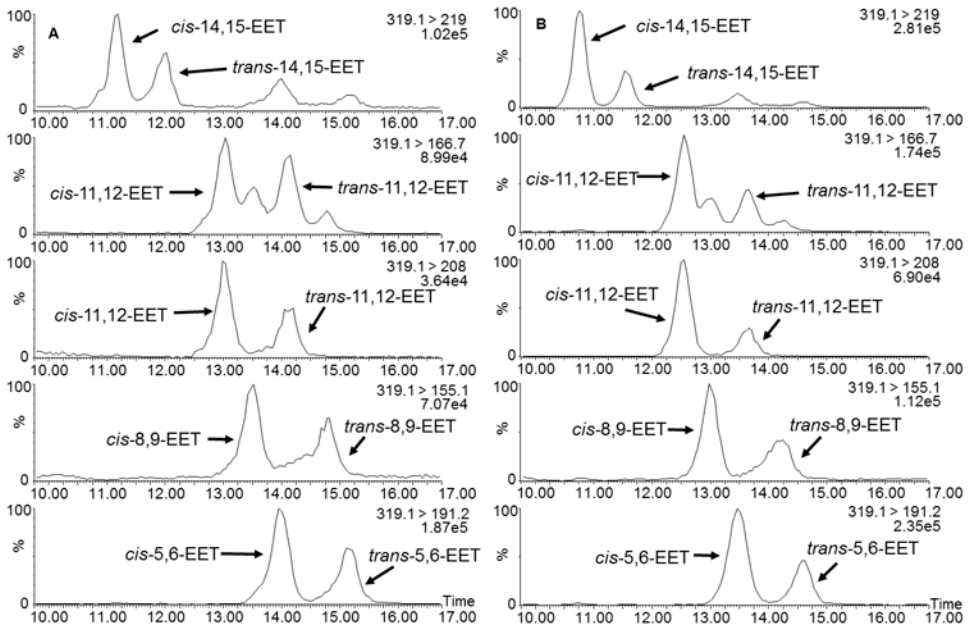

Fig. 6.

Extracted ion chromatograms of EETs extracted from erythrocyte membrane of C57BL/6 mice (A) and human (B). The chromatograms demonstrate separation of *cis*- and *trans*-EETs.

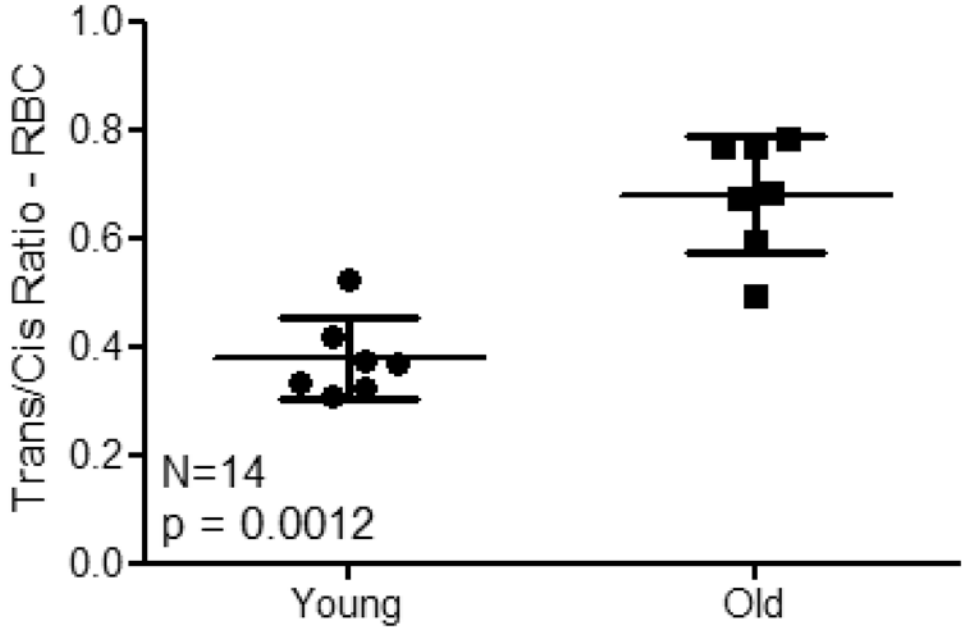

Fig. 7.
Comparison of total *trans/cis*-EETs in RBC of young and old mice.

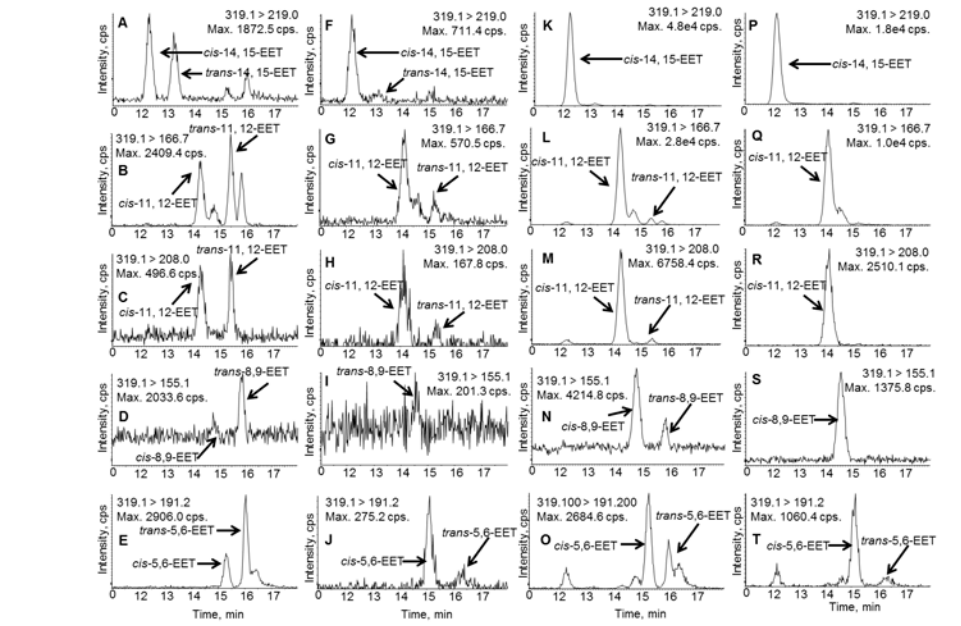

Components				
KPi	+	+	+	+
DETAPAC	-	+	-	+
Pyruvate	-	+	-	+
NADPH	-	-	+	+

Fig. 8.

Extracted ion chromatograms of reconstituted CYP enzyme incubation of AA in the absence and presence of NADPH, DETAPAC, and pyruvate. Formation of non-NADPH-dependent *cis*- and *trans*-EETs was observed at greater intensity in the no NADPH control in potassium phosphate (KPi) buffer (A-E) while addition of DETAPAC and pyruvate markedly reduced NADPH-independent formation of EETs (F-J). In the presence of NADPH and absence of both DETAPAC and pyruvate, *cis*-EETs were observed at a very high level, which confirmed that CYP exclusively make *cis*-EETs (K-O). In this sample, *trans*-EETs were still observed. Addition of DETAPAC and pyruvate markedly diminished the formation of non-NADPH-dependent EETs (P-T). Normalization of EETs formed in the incubation to its corresponding no NADPH control was still necessary for all samples.

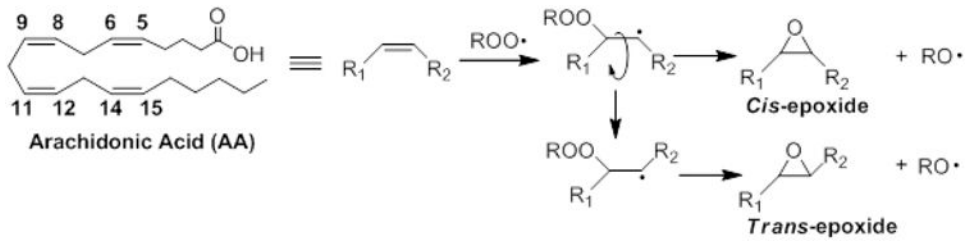

Fig. 9.
Proposed mechanism of *cis*- and *trans*-EET formation via free radical oxidation.

Table 1

Percentages of each *cis*- and *trans*-EET relative to total *cis*- or *trans*-EETs, respectively, in benzene and liposomes

Reaction condition		% 14,15-EET	% 11,12-EET	% 8,9-EET	% 5,6-EET
Benzene	*cis*-	51 ± 2	11 ± 1	19 ± 1	19 ± 3
	trans-	43 ± 4	12 ± 1	22 ± 2	21 ± 3
Liposomes	*cis*-	28 ± 5	9.1 ± 2	27 ± 4	36 ± 9
	trans-	18 ± 3	5.1 ± 0.8	32 ± 3	45 ± 6

Each entry is an average of four concentrations and three time points. Experiments were performed in triplicates and data are presented as mean ± S.D.

Table 2

Normalized peak height ratios and ratios of each cis- and trans-EET in (A) old and (B) young mouse RBC membranes and hearts

A	Mouse RBC (N=7)			Mouse Heart(N=7)		
	cis-	*trans-*	*cis/trans-*	*cis-*	*trans-*	*cis/trans-*
14,15-EET	0.068 ± 0.01	0.035 ± 0.006	2.0 ± 0.2	0.0045 ± 0.0008	0.0038 ± 0.0007	1.2 ± 0.1
11,12-EET	0.081 ± 0.02	0.065 ± 0.02	1.3 ± 0.4	0.0046 ± 0.0009	0.0061 ± 0.001	0.77 ± 0.07
8,9-EET	0.027 ± 0.004	0.019 ± 0.006	1.6 ± 0.5	0.0034 ± 0.0006	0.0080 ± 0.002	0.43 ± 0.05
5,6-EET	0.026 ± 0.006	0.021 ± 0.005	1.3 ± 0.3	0.0025 ± 0.0005	0.0026 ± 0.0005	1.0 ± 0.2

B	Mouse RBC (N=7)			Mouse Heart(N=7)		
	cis-	trans-	cis/trans-	cis-	trans-	cis-/trans-
14,15-EET	0.0079 ± 0.002	0.0030 ± 0.0007	2.6 ± 0.4	0.0037 ± 0.0009	0.0033 ± 0.0008	1.1 ± 0.2
11,12-EET	0.0044 ± 0.001	0.0029 ± 0.0007	1.5 ± 0.2	0.0028 ± 0.0007	0.0031 ± 0.0008	0.9 ± 0.1
8,9-EET	0.019 ± 0.005	0.0073 ± 0.002	2.6 ± 0.5	0.0038 ± 0.0009	0.0093 ± 0.002	0.41 ± 0.06
5,6-EET	0.031 ± 0.009	0.0095 ± 0.002	3.3 ± 0.7	0.0066 ± 0.002	0.012 ± 0.004	0.60 ± 0.2

Mouse RBC membranes were normalized to 30 mg/mL of total protein while mouse heart tissues were normalized to weight.

The data in the table are presented as means ± S.D.

Table 3

Normalized peak height ratios and ratios of each *cis*- and *trans*-EET in human RBC membranes and diseased hearts

	Human RBC (N=28)			Human Heart (N = 12)		
	cis-	***trans-***	***cis-/trans-***	***cis-***	***trans-***	***cis/trans-***
14,15-EET	0.017 ± 0.005	0.0094 ± 0.006	2.0 ± 0.6	0.0033 ± 0.0007	0.0019 ± 0.0007	1.9 ± 0.6
11,12-EET	0.013 ± 0.006	0.010 ± 0.007	1.5 ± 0.5	0.0057 ± 0.001	0.0056 ± 0.002	1.2 ± 0.4
8,9-EET	0.016 ± 0.005	0.010 ± 0.007	1.9 ± 0.6	0.011 ± 0.003	0.0050 ± 0.002	2.3 ± 0.5
5,6-EET	0.014 ± 0.009	0.0076 ± 0.007	2.2 ± 0.9	0.0091 ± 0.004	0.0056 ± 0.002	1.7 ± 0.6

Human RBC membranes were normalized to 50 mg/mL of total protein while heart tissues were normalized to tissue weight.

The data in the table are presented as means ± S.D.

Table 4

Percent remaining of NADPH independent formation of EETs in reconstituted CYP enzyme system according to materials and methods.

Additives	14,15-EET	11,12-EET	8,9-EET	5,6-EET
EDTA	10.3%	14.2%	25.1%	56.3%
DETAPAC	6.5%	9.2%	15.9%	61.9%
EDTA + Pyruvate	4.8%	7.4%	12.2%	29.9%
DETAPAC + Pyruvate	3.2%	4.7%	6.9%	21.3%

Each condition was performed in duplicates.